

Energetics of Primary Charge Separation in Bacterial Photosynthetic Reaction Center Mutants: Triplet Decay in Large Magnetic Fields[†]

Alex de Winter and Steven G. Boxer*

Department of Chemistry, Stanford University, Stanford, California 94305-5080

Received: August 12, 2002

The triplet state of aromatic molecules forms and decays by intersystem crossing, as originally demonstrated by Kasha and Lewis. By contrast, the triplet state of the primary electron donor, ³P, in photosynthetic reaction centers is formed exclusively by spin- and magnetic-field-dependent charge recombination of the initially formed radical ion pair. ³P decays by intersystem crossing at low temperatures; however, at higher temperatures, it can also decay by activated re-formation of the radical ion pair from which it was born, followed by a spin- and magnetic-field-dependent pathway that leads ultimately to the ground state. The discovery of this activated decay pathway leads to an approach for obtaining information on the relative energies of the radical pair and ³P state (Chidsey et al. *Proc. Natl. Acad. Sci. U.S.A.* **1985**, 82, 6850–6854); with knowledge of the absolute energy of ³P from its phosphorescence, the energy of the initial charge separation reaction can be obtained. In this paper, we present the first data on the temperature and magnetic field dependence of the formation and decay of ³P for *Rb. sphaeroides* reaction center mutants in a background that contains no carotenoid. The mutations have been studied in other contexts and were designed to perturb the redox potential of the primary electron donor or acceptor. The measured trends are in the same direction as expected from chemical intuition; however, the quantitative changes are typically smaller than expected. Possible reasons for this finding are discussed. Improved values are obtained for the enthalpy and free energy change associated with primary charge separation in wild-type reaction centers.

Introduction

The energetics of the initial electron-transfer steps in bacterial photosynthetic reaction centers (RCs) is a key element in any attempt to understand the reaction mechanism and the impact of amino acid changes, temperature, and applied electric fields on the reaction. The organization of the chromophores involved in energy and electron transfer along with the sites of mutations considered in the following are shown in Figure 1. A kinetic scheme describing charge separation and recombination when electron transfer to quinone Q_A is blocked is shown in Figure 2. The enthalpy and free energy changes for the initial process ${}^1\text{P} \rightarrow \text{P}^+\text{H}_\text{L}^-$ are difficult to obtain reliably in situ. Although the P/P⁺ oxidation potential can be measured in situ, there is no reliable way to obtain the H_L/H_L⁻ reduction potential. Furthermore, it is not certain that the equilibrium P/P⁺ potential is the relevant quantity for the picosecond to nanosecond time scale processes sketched in Figure 2, as the time scale for solvation of the nascent ions is not well understood.

Two separate approaches were developed several years ago to obtain information on the energetics in situ: measurements of the amplitude of delayed fluorescence from ¹P following activated charge recombination, $\text{P}^+\text{H}_\text{L}^- \rightarrow {}^1\text{P}$,^{2–7} and the activation energy of the reaction ${}^3\text{P} \rightarrow \text{P}^+\text{H}_\text{L}^-$,^{1,8} combined with information on the ³P energy from phosphorescence measurements.⁹ The results obtained differ substantially both in the absolute value of the ${}^1\text{P} \rightarrow \text{P}^+\text{H}_\text{L}^-$ free energy change and in the contributions to this change from enthalpy and entropy.

[†] Part of the special issue “George S. Hammond & Michael Kasha Festschrift”.

* Corresponding author: Steven G. Boxer. E-mail: Sboxer@Stanford.edu. Phone: (650) 723-4482. Fax: (650) 723-4817.

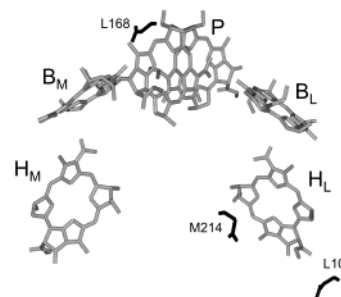


Figure 1. Arrangement of the chromophores involved in the initial electron transfer in photosynthetic reaction centers. Amino acid residues that were mutated for this study are included in the figure.

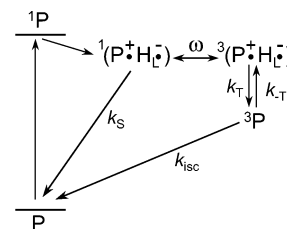


Figure 2. Reaction scheme depicting electron transfer as well as the formation and decay of ³P. The vertical positions of the species indicate their relative free energies, although the figure is not to scale.

Some of this difference might result from the time scales sampled, but there might be shortcomings of each approach as well, as discussed below.

In the following, we describe measurements using the temperature and magnetic field dependence of the triplet decay rate in a series of mutants that have been designed to perturb the energetics of charge separation. This approach was originally

applied to RCs from the carotenoidless *Rb. sphaeroides* R26 strain,⁸ but it could not be applied to RC mutants, as they were originally prepared in a carotenoid-containing strain and the carotenoid rapidly quenches ³P. Recently, a *Rb. sphaeroides* RC mutant, M71GL, has been described that assembles without carotenoid,¹⁰ so that experiments that depend on ³P can be undertaken. In the following, we report the temperature and magnetic field dependence of the triplet decay of a series of RC mutants in the M71GL background to obtain information on the energetics of the initial charge separation reaction.

Principle of Method. As diagrammed in Figure 2, when Q_A is either removed or chemically reduced, the singlet radical pair ¹(P⁺H_L⁻) can either decay to the ground state with rate *k_S*, undergo activated charge recombination to re-form ¹P (the basis of the delayed fluorescence approach), or undergo coherent spin evolution, with frequency *ω*, to form the triplet spin configuration of the radical pair, ³(P⁺H_L⁻). ³(P⁺H_L⁻) decays either by charge recombination to form ³P with rate *k_T* or by spin evolution to re-form ¹(P⁺H_L⁻).¹¹ In RCs lacking carotenoid, ³P decays by intersystem crossing with rate *k_{isc}*, or it can re-form the state from which it came by the thermally activated rate *k_{-T}*, demonstrated by the magnetic field effect on the ³P decay rate.¹ The activation energy of the latter process provides information on the energetics of charge separation when combined with spectroscopic data on the energies of ¹P and ³P.⁹

In quinone-depleted RCs, used to avoid further complications involving spin exchange between H_L⁻ and Q_A⁻,¹² within 100 ns of the excitation of P, the RCs have either returned to the ground state or formed the ³P state. The triplet quantum yield, Φ_{3P}, and the decay kinetics of ³P can be measured by monitoring the ground-state recovery of P. As discussed in detail elsewhere,¹ the temperature dependence of the observed triplet decay rate *k_{obs}* is given by

$$k_{\text{obs}} = k_{\text{isc}} + \alpha e^{-\Delta H^\circ \beta} \quad (1)$$

where

$$\alpha = \frac{1}{3} k_S \Phi_{3P} e^{\Delta S^\circ / k_B} \quad (2)$$

and Δ*H*[°] and Δ*S*[°] are the standard enthalpy and entropy differences, respectively, between ³P and ³(P⁺H_L⁻); β is 1/*k_BT*, where *k_B* is the Boltzmann constant; and *T* is the absolute temperature. At zero or low applied magnetic field, singlet–triplet interconversion is driven by the nuclear hyperfine interaction,^{13,14} whereas at high field, the difference in *g* factors of the radicals, Δ*g*, dominates singlet–triplet mixing.¹⁵ At low field, the subpopulation of RCs whose nuclear spins generate a large hyperfine field will have larger values of *ω* and will evolve more rapidly to ³(P⁺H_L⁻). Thus, the nuclear hyperfine-induced singlet–triplet radical pair interconversion enriches ³P with nuclear spin states that generate large hyperfine fields, resulting in nuclear spin polarization.¹⁶ Because equilibration of nuclear spin states (spin lattice relaxation) might be on the same time scale or slower than the lifetime of ³P, subsequent decay through ³(P⁺H_L⁻) via *k_{-T}* might be faster because of a larger *ω* than it would be if the nuclear spins were at thermal equilibrium.¹⁷ As a result, *k_{obs}* is greater than it would be with an equilibrium population of nuclear spins, as was assumed in the derivation of eq 1. The extrapolated activation energy from the low- or zero-field measurements is then smaller than it should be, making the apparent enthalpy difference between ¹P and ¹(P⁺H_L⁻) larger than it actually is.¹⁸ To minimize this problem,

the experiment is carried out in the highest possible applied magnetic field so that nuclear spins play a smaller part in singlet–triplet mixing.⁸ Ideally, one would like to work in the “infinite-field limit,” where singlet–triplet mixing effectively equilibrates ¹(P⁺H_L⁻) and ³(P⁺H_L⁻), although it might be impractical to achieve such fields depending on the values of *k_S*, *k_T*, and Δ*g*.

Equation 1 provides an alternative method of determining the activation energy for ³P → ³(P⁺H_L⁻). Because an applied magnetic field can vary the value of *ω* by the Δ*g* effect, the quantum yield of triplet formation is magnetic-field-dependent. Combining the enthalpy and entropy terms, one can rewrite eq 1 as

$$k_{\text{obs}} = k_{\text{isc}} + \frac{1}{3} k_S \Phi_{3P}(B) e^{-\Delta G^\circ \beta} \quad (3)$$

where Δ*G*[°] is the standard free energy of the reaction and Φ_{3P}(*B*) is the triplet quantum yield at applied magnetic field *B*. The absolute magnitude of the triplet yield at any magnetic field, Φ_{3P}(*B*), is not simple to measure accurately; however, the triplet yield at a given magnetic field *B* relative to the triplet yield at zero field, Φ_{3P}(*B*)/Φ_{3P}(*B*=0), is straightforward to measure by taking the ratio of the initial bleach of P at magnetic field *B* relative to that at *B* = 0. A plot of *k_{obs}* vs Φ_{3P}(*B*)/Φ_{3P}(*B*=0) has a *y* intercept of *k_{isc}* and a slope of

$$\text{slope} = \frac{1}{3} k_S \Phi_{3P}(B=0) e^{-\Delta G^\circ \beta} \quad (4)$$

If the values of *k_S* and Φ_{3P}(*B*=0) are known, the free energy difference between ³P and ³(P⁺H_L⁻) can be determined. By comparing Δ*H*[°] with Δ*G*[°], the contribution of Δ*S*[°] can be obtained. Although the values of *k_S* and Φ_{3P}(*B*=0) are known quite accurately for R26 RCs, they have not been measured for most of the mutants used in this study. Nonetheless, we report data obtained in this way and provide some preliminary analysis given available information.

Choice of Mutants. In the following, we consider four mutants, the M71GL carotenoidless mutant for comparison with R26 RCs and three double mutants in the M71GL background: L168HF, L104EV, and M214LH (the beta mutant). The L168HF mutation is designed to modify the environment of P by removing a hydrogen-bonding group near the ring I acetyl group of the L-side chromophore of the special pair.¹⁹ This has been shown to decrease the oxidation potential of P, thereby altering the energetics of electron transfer; L168HF is the single hydrogen-bond mutation that results in the largest decrease in the P/P⁺ potential.²⁰ The L104EV mutation removes a hydrogen bond from the 9-keto carbonyl group of the H_L chromophore.²¹ Removing the hydrogen bond should raise the reduction potential of the H_L bacteriochlorophyll. The M214LH mutation replaces a noncoordinating leucine with a histidine over the center of the H_L chromophore. This RC assembles with a bacteriochlorophyll in the H_L binding site, and this new chromophore is called β_L.²² Because bacteriochlorophyll has a substantially higher reduction potential *in vitro* than bacteriochlorophyll, the driving force for initial electron transfer should be decreased.

Experimental Section

All of the mutants were constructed with a PCR-based mutagenesis kit, followed by excision and ligation of the relevant restriction fragments. The following *Rb. sphaeroides* mutants were created: M71GL, M71GL/L168HF, M71GL/L104EV, and

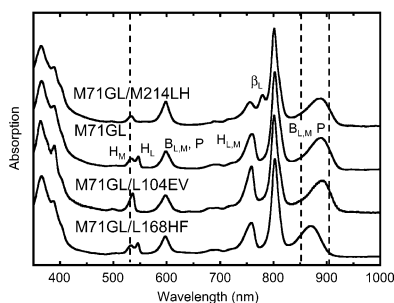


Figure 3. Low-temperature (77 K) absorption spectra of the mutants made for this study. The RCs are suspended in 60% glycerol, and the spectra are normalized to the same absorption at 802 nm. The three dotted lines indicate the excitation wavelength (532 nm), and the probe wavelengths (852 and 905 nm).

M71GL/M214LH. The mutations were inserted into a plasmid that produces RCs with a polyhistidine tag for rapid purification.²³ Following purification, RCs were suspended in 10 mM Tris-HCl (pH 8.0), 0.1% LDAO, 1.0 mM EDTA. Q_A was removed by standard procedures,²⁴ and the RCs were mixed with glycerol to a final glycerol concentration of 60%.

For high magnetic field measurements, the RCs were placed in a 3-mm-path-length glass cuvette. The cuvette was mounted on a copper block, which was cooled by a jet of helium gas. The temperature of the helium gas jet could be varied with a heater and was monitored with a Cernox resistance temperature sensor. As a secondary temperature control, the temperature of the copper block was measured with a platinum resistance sensor and was varied with a Kapton film heater. The sample was placed in an Oxford Instruments superconducting Spectromag system, with variable magnetic field up to 8 T. The split-bore Spectromag allowed for a perpendicular pump/probe excitation geometry.

For measurements of transient absorption kinetics, the sample was excited with a subsaturating 532-nm actinic pulse (fwhm \approx 8 ns) from a Nd:YAG laser at a 2-Hz repetition rate. The time dependence of the bleach of the P ground state (which is a measure of the relative concentration of 3P) was monitored with a weak probe laser diode at 852 or 905 nm and detected with a fast photodiode and a digital oscilloscope. Data were taken with the probe beam polarized at the magic angle with respect to the magnetic field direction. The absorbance change was linear with respect to pump power and independent of probe power. The Q-depletion procedure is not perfect, so there is a small population (generally less than 10%) of the RCs that still contains quinone. This results in a bleach component that decays on a 100-ms time scale, about 3 orders of magnitude longer than the decay of 3P . This is accounted for by fitting the microsecond decay curves with a small baseline offset.

For low magnetic field experiments, the sample was cooled with a miniature Joule–Thompson refrigerator (MMR Technologies) with precise temperature control from 300 to 117 K. The magnetic field was generated with a Helmholtz electromagnet driven by a 1-kW current-regulated power supply, resulting in a variable magnetic field from 0 to 400 G.

Results

The low-temperature absorption spectra for all four mutants are shown in Figure 3. The absence of carotenoid in the RCs is evidenced by the lack of the broad absorption between 400 and 550 nm attributable to the carotenoid. Note that the absorption at 532 nm, the wavelength of excitation for the transient absorption experiments, differs among the mutants. To roughly

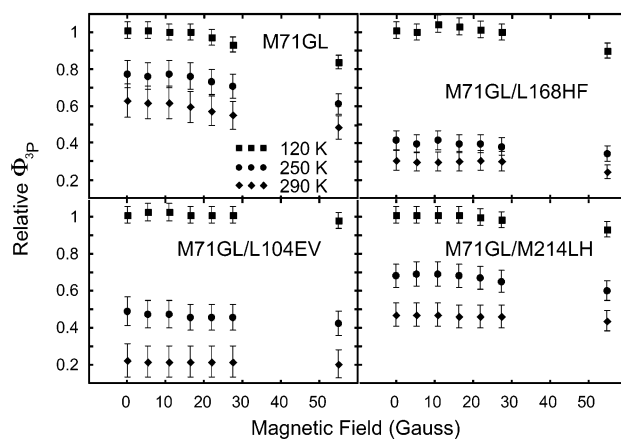


Figure 4. Relative quantum yield of 3P as a function of magnetic field, normalized to 1 for each mutant with zero applied field at 120 K. Data were taken at 120, 250, and 290 K, as indicated. Vertical axes are scaled to facilitate side-by-side comparison.

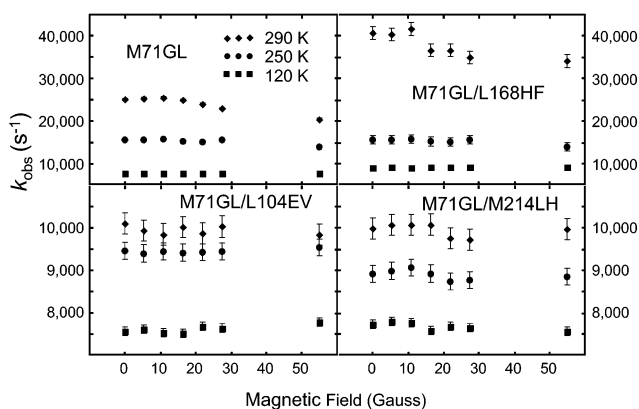


Figure 5. k_{obs} as a function of low magnetic field for all four mutants at 290, 250, and 120 K, as indicated. The vertical axes are scaled to facilitate side-by-side comparison.

compare relative triplet yields between the mutants, the experimental sample concentrations were adjusted such that the absorption at 532 nm was approximately the same.

The time dependence of the bleach in the P absorption on the μs time scale can be fit well by a single exponential along with a small baseline offset, reflecting the fraction of RCs that still contain quinone. The initial bleach amplitude reflects the relative triplet yield as 3P does not absorb appreciably at 852 or 905 nm. By using 532-nm excitation pulses, photoselection/polarization effects are minimized.²⁵ For each mutant, an analysis of 3P amplitude and decay was performed as a function of temperature and magnetic field. The relative triplet yield and k_{obs} value for each mutant at low magnetic fields and three different temperatures are shown in Figures 4 and 5, and the relative triplet yields at room temperature and high magnetic fields are plotted in Figure 6. The temperature dependences of k_{obs} at 8 T are shown in Figures 7–10, along with fits to eq 1. The compiled results for the temperature-dependent data are summarized in Table 1, and a schematic of ΔH° for $^3P \rightarrow ^3(P^+H_L^-)$ for all four mutants is shown in Figure 11.

Generally, the temperature-dependent data at 8 T have small error bars and fit well to eq 1. Each data point is the average of three measurements, and the vertical error bars, indicating the standard deviation of k_{obs} , are small; the error in temperature for each measurement is smaller than the data points. The M71GL/L104EV and M71GL/M214LH mutants were more difficult to study than the other mutants. The M71GL/L104EV mutant is considerably less stable than the other double

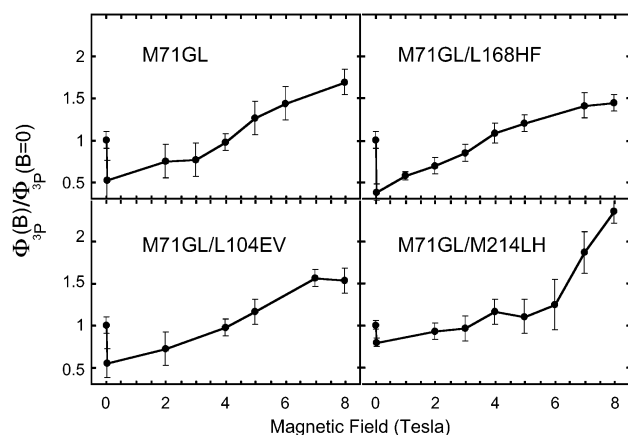


Figure 6. Room-temperature quantum yield of ^3P formation at an applied field [$\Phi_{3\text{P}}(B)$] relative to the quantum yield of ^3P formation at zero field [$\Phi_{3\text{P}}(B=0)$] plotted against applied magnetic field.

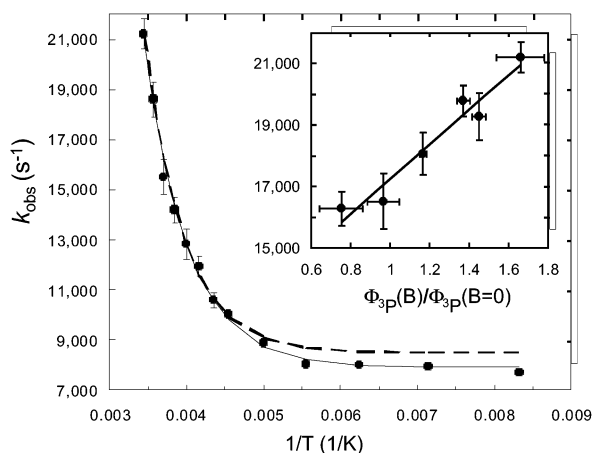


Figure 7. Temperature dependence of k_{obs} for M71GL at an applied field of 8 T. The solid line is the fit to M71GL data, and the dashed line is fit to R26 data (see text). Data fit to an exponential with $k_{\text{isc}} = 7900 \pm 150 \text{ s}^{-1}$, $a = (6.0 \pm 1.5) \times 10^6 \text{ s}^{-1}$, and $\Delta H^\circ = 1230 \pm 60 \text{ cm}^{-1}$. Inset: M71GL k_{obs} plotted as a function of relative triplet yield at 290 K. Data fit to a straight line with slope = $5600 \pm 1100 \text{ s}^{-1}$ and intercept = $11\,700 \pm 1500 \text{ s}^{-1}$.

mutants: the protein yield per gram of cells is about half that for the other mutants, and a large fraction of the M71GL/L104EV RCs denature upon quinone depletion. The L104 site is close to the Q_A binding pocket, and it is possible that the combination of removing the hydrogen bond to H_L and removing the quinone is enough of a perturbation to destabilize the protein structure. The end result is that it proved difficult to obtain enough Q-depleted protein to carry out experiments, and combined with a low triplet yield (see below), this resulted in a poorer signal-to-noise ratio for this mutant than for the others. The ground-state bleach of P is significantly smaller in M71GL/M214LH than in any of the other mutants, indicating a much lower triplet yield, and resulting in a poor signal-to-noise ratio. The low triplet yield is likely due to the fact that $^1(\text{P}^+\beta_\text{L}^-)$ recombination is nearly 20 times faster than for wild-type,²² leaving insufficient time for significant singlet–triplet evolution by any mechanism. The g factor for β_L^- has not been reported, as it is difficult to trap given the short $\text{P}^+\beta_\text{L}^-$ lifetime.²⁶ The in vitro g factor for the bacteriochlorophyll radical anion (2.0028 ± 0.0002)^{27,28} is comparable to that for the bacteriopeophytin radical anion (2.0031 ± 0.0002).^{28–30}

The values of k_{obs} versus the quantum yield of ^3P normalized relative to the yield at zero field as a function of magnetic field at room temperature are shown in the insets for each mutant in

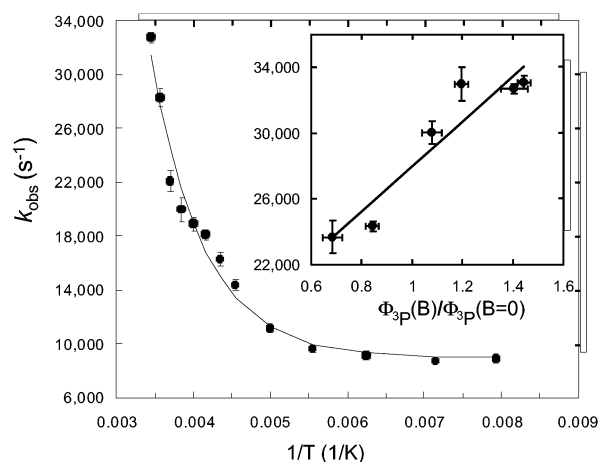


Figure 8. Temperature dependence of k_{obs} for M71GL/L168HF at an applied field of 8 T. Data fit to an exponential with $k_{\text{isc}} = 8900 \pm 600 \text{ s}^{-1}$, $a = (3.5 \pm 1.9) \times 10^6 \text{ s}^{-1}$, and $\Delta H^\circ = 1020 \pm 100 \text{ cm}^{-1}$. Inset: M71GL/L168HF k_{obs} plotted as a function of relative triplet yield at 290 K. Data fit to a straight line with slope = $13\,700 \pm 1700 \text{ s}^{-1}$ and intercept = $14\,000 \pm 2000 \text{ s}^{-1}$.

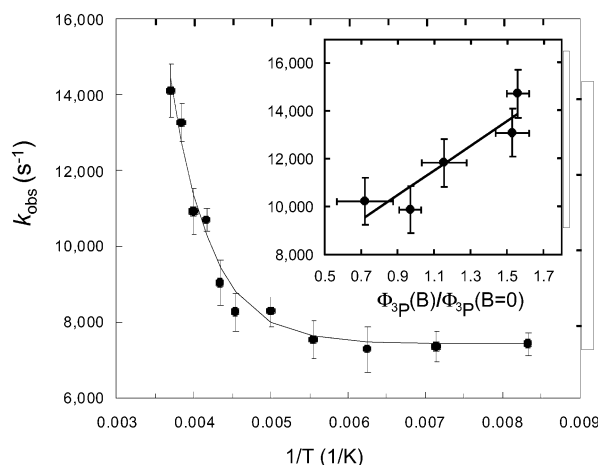


Figure 9. Temperature dependence of k_{obs} for M71GL/L104EV at an applied field of 8 T. Data fit to an exponential with $k_{\text{isc}} = 7300 \pm 200 \text{ s}^{-1}$, $a = (9.6 \pm 8.0) \times 10^6 \text{ s}^{-1}$, and $\Delta H^\circ = 1360 \pm 150 \text{ cm}^{-1}$. Inset: M71GL/L104EV k_{obs} plotted as a function of relative triplet yield at 290 K. Data fit to a straight line with slope = $5000 \pm 2000 \text{ s}^{-1}$ and intercept = $5800 \pm 2500 \text{ s}^{-1}$.

Figures 7–10. The ordinate for each point is k_{obs} for a particular magnetic field B , and the abscissa is $\Phi_{3\text{P}}(B)/\Phi_{3\text{P}}(B=0)$. Because there is error both in the measurement of the zero-field triplet yield (calculated from the initial bleach amplitude, transmission prior to the pump pulse, and sample absorption) and in the relative triplet yield at the applied magnetic field, the horizontal error bars in the insets of Figures 7–10 tend to be large. In the previous iteration of these experiments on the R26 RCs, Goldstein et al. used a 13.5-T magnet.⁸ The consequence of using a weaker magnet for the current set of measurements is that there is a smaller range over which to extrapolate a linear relationship between k_{obs} and $\Phi_{3\text{P}}(B)/\Phi_{3\text{P}}(B=0)$. In the case of the M71GL/M214LH and M71GL/L104EV mutants, where the triplet yields are very low, there is a large error in the zero-field value, giving rise to especially large error in the relative triplet yield. The parameters from the linear fits to the insets in Figures 7–10 are summarized in Table 2.

Discussion

Approaches to Data Analysis. The validity of eq 1 for determining ΔH° for $^3\text{P} \rightarrow ^3(\text{P}^+\text{H}_\text{L}^-)$ from the temperature

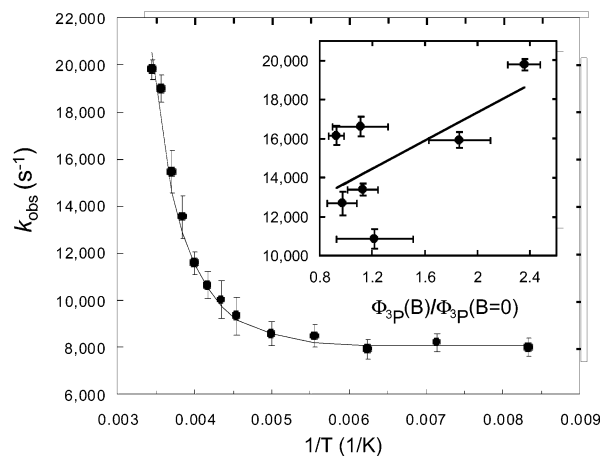


Figure 10. Temperature dependence of k_{obs} for M71GL/M214LH at an applied field of 8 T. Data fit to an exponential with $k_{\text{isc}} = 8000 \pm 300 \text{ s}^{-1}$, $a = (15 \pm 12) \times 10^6 \text{ s}^{-1}$, and $\Delta H^\circ = 1440 \pm 200 \text{ cm}^{-1}$. Inset: M71GL/214LH k_{obs} plotted as a function of relative triplet yield at 290 K. Data fit to a straight line with slope = $3600 \pm 1900 \text{ s}^{-1}$ and intercept = $10\,000 \pm 2800 \text{ s}^{-1}$.

dependence of the triplet decay has been discussed previously.^{1,8} Briefly, the analysis is predicated on the assumption that k_{S} , k_{isc} , ΔH° , ΔS° , and $\Phi_{3\text{P}}$ are temperature-independent. For R26 reaction centers, k_{S} and $\Phi_{3\text{P}}$ do depend on temperature, with k_{S} decreasing by a factor of about 4 as the temperature is lowered from room temperature to 120 K³¹ and $\Phi_{3\text{P}}$ increasing by a factor of approximately 3 over the same range.³² The temperature dependences of these two factors are related: as k_{S} decreases, the triplet-forming pathway competes more effectively with charge recombination to the ground state (Figure 2). The temperature dependences of these parameters have not yet been reported for any of the double mutants made for this study, but it is reasonable to assume that, given the underlying scheme, the temperature dependences will generally offset, so that the product, $k_{\text{S}}\Phi_{3\text{P}}$, will be only weakly temperature-dependent and much less so than the exponential dependence in the activation term.

The magnetic field dependence of k_{obs} and the triplet quantum yield is a second method for determining the activation energy for ${}^3\text{P} \rightarrow {}^3(\text{P}^+\text{H}_\text{L}^-)$. To extract any useful information from the fit, k_{S} and $\Phi_{3\text{P}}(B=0)$ for each mutant must be known. k_{S} has not been directly measured for any of the mutants studied, although the radical pair lifetime has been measured for Q-depleted L168HF and M214LH mutants of *Rb. sphaeroides*.^{33,34} $\Phi_{3\text{P}}(B=0)$ is known with reasonable accuracy for R26 reaction centers, and this value should apply to M71GL (see below), but $\Phi_{3\text{P}}(B=0)$ has not been measured for any of the other mutants studied. To estimate $\Phi_{3\text{P}}(B=0)$ for a mutant, we compare the initial bleach of P in the mutant with that of M71GL, using samples with the same absorption at 532 nm and taking into account the probe transmission prior to the excitation pulse and the sample absorption at the probe wavelength (Figure 3). Substituting the slope of the fit line, k_{S} , and $\Phi_{3\text{P}}(B=0)$ into eq 4 gives the experimental value of ΔG° , the standard free energy difference between ${}^3\text{P}$ and ${}^3(\text{P}^+\text{H}_\text{L}^-)$.

M71GL. M71GL is the background mutation that makes these experiments possible, and it is important to compare M71GL and R26 RCs. The value of k_{obs} and its dependence on a small applied field, as well as the dependence of the relative triplet yield on a small magnetic field, are very similar to those of R26 RCs (Figures 4 and 5).¹ $\Phi_{3\text{P}}$ decreases with increasing field at all temperatures (Figure 4), as the applied field breaks

the near energetic degeneracy of the singlet and triplet radical pair states, thereby decreasing interconversion between the states. k_{obs} is affected by an applied field only at higher temperatures (Figure 5): once in the ${}^3\text{P}$ state, the RC requires sufficient thermal energy to re-form ${}^3(\text{P}^+\text{H}_\text{L}^-)$ and thereby decay through the process that is affected by an applied magnetic field.

In the earlier experiments on the temperature dependence of k_{obs} for R26 RCs at high magnetic field, the experimental apparatus did not allow the sample temperature to be lowered below 200 K, and this was used to provide the asymptotic value of k_{isc} .⁸ In these new measurements, we were unable to apply such high magnetic fields, but were able to lower the temperature to 1.5 K (120 K proves adequate). As shown in Figure 7 (dashed line), the single-exponential fit for the high-magnetic-field data points from 290 to 200 K used in the earlier work on R26 ($\Delta H^\circ = 1450 \text{ cm}^{-1}$) fits well to the new data on M71GL over the temperature range 290–200 K; however, it does not adequately fit all of the points in the low-temperature region. If the 8-T field applied in the current experiments were not sufficiently close to the infinite-field limit to circumvent the effects of nuclear spin polarization, the high-temperature points in the current data set would deviate from those of the previous data set with the 13.5-T magnet. The observation that they do not suggests that the 8-T magnet is able to drive the radical pair singlet–triplet interconversion through the Δg effect, with minimal perturbation from the effects of nuclear spin polarization.

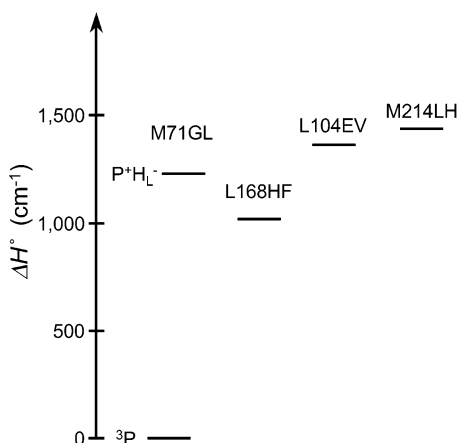
With the wider temperature range, we can refine the value of ΔH° . Figure 7 (solid line) shows the single-exponential fit over the entire temperature range and gives $\Delta H^\circ = 1230 \text{ cm}^{-1}$. With this improved value for the activation energy for ${}^3\text{P} \rightarrow {}^3(\text{P}^+\text{H}_\text{L}^-)$, the enthalpy difference between ${}^1\text{P}$ and ${}^1(\text{P}^+\text{H}_\text{L}^-)$ increases from the previous value of 2050 to 2270 cm^{-1} . The preexponential decreases by a factor of 2 in the full fit relative to the 290–200 K fit for data taken at 13.5 T. The fit to the larger range of temperature points results in a better determination of the preexponential, although some of the difference between the preexponential from this fit and the 13.5-T fit is due to the fact that the triplet quantum yield at 8 T is about 20% less than that at 13.5 T.⁸

The values of k_{obs} as a function of the relative ${}^3\text{P}$ quantum yield between 2 and 8 T at room temperature fit reasonably well to a line (Figure 7, inset). From eq 3, the y intercept of the line is k_{isc} . k_{isc} is known to have some dependence on temperature,¹ and it is reasonable that the value derived from this room-temperature measurement is not identical to the low-temperature limiting value of k_{obs} . The slope of the fit line, 5600 s^{-1} , is equal to $1/3 k_{\text{S}} \Phi_{3\text{P}}(B=0) e^{-\Delta G^\circ/\beta}$. The value of k_{S} for R26 RCs (and presumably M71GL) has been measured to be $(4.9 \pm 0.4) \times 10^7 \text{ s}^{-1}$,³⁵ and $\Phi_{3\text{P}}(B=0)$ for R26 RCs has been determined to be 0.32 ± 0.04 ,^{12,35} so the value for ΔG° for ${}^3\text{P} \rightarrow {}^3(\text{P}^+\text{H}_\text{L}^-)$ is $1390 \pm 40 \text{ cm}^{-1}$. The resulting free energy difference for initial electron transfer in M71GL derived from the magnetic-field-dependent data is 2110 cm^{-1} . As in our earlier work, within the experimental error, the value of ΔG° is approximately equal to that of ΔH° .

The driving force for the reaction ${}^1\text{P} \rightarrow {}^1(\text{P}^+\text{H}_\text{L}^-)$ has also been estimated by redox potentials and delayed fluorescence. Comparisons between redox measurements, delayed fluorescence, and triplet decay measurements have been discussed previously; see Goldstein et al.⁸ or Parson³⁶ for reviews. Redox measurements suggest that $\text{P}^+\text{H}_\text{L}^-$ is $8430\text{--}8510 \text{ cm}^{-1}$ ($1045\text{--}1055 \text{ meV}$) above the ground state and $2690\text{--}2770 \text{ cm}^{-1}$ below ${}^1\text{P}$.^{20,29,33,37–41} Analysis of the amplitude of delayed fluorescence

TABLE 1: Fit Parameters from the Temperature-Dependent, High-Magnetic-Field Data

mutant	$k_{\text{isc}}, \text{s}^{-1}$	α, s^{-1}	$\Delta H^\circ \text{}^3\text{P} \rightarrow \text{}^3(\text{P}^+\text{H}_\text{L}^-), \text{cm}^{-1}$
M71GL	7900 ± 150	$(6.0 \pm 1.5) \times 10^6$	1230 ± 60
M71GL/L168HF	8900 ± 600	$(3.5 \pm 1.9) \times 10^6$	1020 ± 100
M71GL/L104EV	7300 ± 200	$(9.6 \pm 8.0) \times 10^6$	1360 ± 150
M71GL/M214LH	8000 ± 300	$(15 \pm 12) \times 10^6$	1440 ± 200

**Figure 11.** Summary schematic depicting the measured enthalpy difference between ${}^3\text{P}$ and $\text{P}^+\text{H}_\text{L}^-$ for the four mutants studied.

for wild-type and R26 RCs yields an apparent free energy difference between ${}^1\text{P}$ and $\text{P}^+\text{H}_\text{L}^-$ of about 1370 cm^{-1} at room temperature, decreasing to 400 cm^{-1} at 100 K .²⁻⁷ Unfortunately, in most measurements of delayed fluorescence because the original papers, magnetic field effects were not reported. We take the presence of a magnetic field effect as an essential indication that the species giving rise to delayed fluorescence (or the back-reaction from ${}^3\text{P}$, as in the current work) is a weakly coupled radical pair.

Two other groups have recently obtained estimates for the driving force for initial electron transfer by a combination of transient absorption spectroscopy and simulations. Holzwarth and Müller measured femtosecond transient absorption spectra from 500 to 940 nm over the range 0 – 700 ps and fit the resulting spectra with decay-associated difference spectra (DADS) and species-associated difference spectra (SADS).⁴² They modeled these spectra extensively and, from the kinetic models, determined that the room-temperature free energy difference between ${}^1\text{P}$ and $\text{P}^+\text{H}_\text{L}^-$ is 730 cm^{-1} and that $\text{P}^+\text{B}_\text{L}^-$ is 330 cm^{-1} below ${}^1\text{P}$. Holzwarth and Müller did not measure the temperature dependence of ΔG° nor did they study RC mutants. They argue that the discrepancy between their measurements and those of Ogrodnik et al. and Goldstein et al. was due to the difference in time scales measured in the experiments. Whereas the experiments of Holzwarth and Müller measured electron transfer on the picosecond scale, the other measurements were slow enough to allow the protein time to relax around the radical pair, lowering its energy. They suggested that this conformational relaxation occurs on the tens to hundreds of picosecond time scale.

In the second alternative method, Volk et al. measured the magnetic field dependence of the reaction yield (MARY), with relatively weak magnetic fields of $\leq 700 \text{ G}$.⁴³ By modeling their transient absorption data, they extract the energies of $\text{P}^+\text{B}_\text{L}^-$ and $\text{P}^+\text{H}_\text{L}^-$. They found that the free energy difference between ${}^1\text{P}$ and $\text{P}^+\text{H}_\text{L}^-$ is $2020 \pm 80 \text{ cm}^{-1}$ and that $\text{P}^+\text{B}_\text{L}^-$ is $570 \pm 80 \text{ cm}^{-1}$ below ${}^1\text{P}$. Their measurements between 200 and 300 K indicate that ΔG° is almost temperature-independent over this range. Volk et al. suggested that the discrepancy between their measurements and fluorescence decay measurements, as well

as those of Holzwarth and Müller, was due to energetic heterogeneity persisting on the hundreds of microsecond time scale. They pointed out that Holzwarth and Müller analyzed their data using decay components with linked amplitudes taken from delayed fluorescence measurements, so that it was not surprising that the results of Holzwarth and Müller resembled those of delayed fluorescence measurements.

The results for the triplet decay experiments reported here for M71GL are very similar to those previously reported for R26. The free energy change for primary charge separation determined from these measurements is larger (2110 cm^{-1}) than the values estimated from delayed fluorescence (1370 – 400 cm^{-1}), and an additional disagreement exists over the role of ΔS° in charge separation. The delayed fluorescence measurements suggest that the charge separation reaction is largely driven by entropy, whereas the triplet decay experiments suggest that the change in entropy associated with charge separation is negligible. There are two recurring explanations for the disagreements between the conclusions reached by delayed fluorescence and triplet decay measurements.³⁶ The disagreement could stem from the fact that delayed fluorescence measurements sample the system during the 20 -ns lifetime of $\text{P}^+\text{H}_\text{L}^-$, whereas the triplet decay measurements cover the 100 - μs lifetime of ${}^3\text{P}$. Thus, the triplet decay and the delayed fluorescence experiments could be measuring the energies of different states or states with differing degrees of relaxation. The second explanation offered is that inhomogeneous broadening, due to different protein conformations, causes the RCs to be heterogeneous with respect to the energy of $\text{P}^+\text{H}_\text{L}^-$.^{7,43} At low temperature, $\text{P}^+\text{H}_\text{L}^-$ will recombine to ${}^1\text{P}$ only in that subpopulation of RCs that has a relatively high energy of $\text{P}^+\text{H}_\text{L}^-$. Persistent energetic inhomogeneity (on the order of $100 \mu\text{s}$) might affect the triplet decay measurements in a similar manner, except that, at low temperature, ${}^3\text{P}$ will re-form ${}^3(\text{P}^+\text{H}_\text{L}^-)$ only in the subpopulation of RCs with a relatively low energy of $\text{P}^+\text{H}_\text{L}^-$. This would cause delayed fluorescence measurements to underestimate the free energy difference between ${}^1\text{P}$ and $\text{P}^+\text{H}_\text{L}^-$ and triplet decay experiments to overestimate the enthalpy difference between ${}^1\text{P}$ and $\text{P}^+\text{H}_\text{L}^-$. This issue is discussed further below.

M71GL/L168HF. The M71GL/L168HF mutant introduces a perturbation to the special pair by removing a hydrogen-bonding group near the ring I acetyl group of the L-side P chromophore. The special pair Q_Y band shifts to 850 nm at room temperature, compared to 865 nm in wild-type (WT). The fluorescence spectrum for L168HF has not been reported, but room-temperature decay-associated spectra from stimulated emission measurements suggest that the emission from L168HF is blue-shifted relative to that of WT.¹⁹ Assuming that the emission is blue-shifted as much as the absorption, the shift in the absorption maximum represents an increase of 200 cm^{-1} in the energy of ${}^1\text{P}$ in the L168HF mutant. At 77 K , the absorption band for M71GL/L168HF shifts to 870 nm , compared with 890 nm for M71GL (an increase of about 260 cm^{-1} relative to M71GL at 77 K) (Figure 3). Phosphorescence has not been measured to determine whether the energy of ${}^3\text{P}$ also shifts in the L168HF mutant; in the absence of precise information, we will assume that the ${}^1\text{P}$ – ${}^3\text{P}$ singlet–triplet splitting is the same as in R26.

TABLE 2: Fit Parameters from the Magnetic-Field-Dependent, Room-Temperature Data

mutant	$k_{\text{isc}}, \text{s}^{-1}$	slope, s^{-1}	$\Delta G^\circ \text{}^3\text{P} \rightarrow \text{}^3(\text{P}^+\text{H}_\text{L}^-), \text{cm}^{-1}$
M71GL	$11\,700 \pm 1500$	5600 ± 1100	1390 ± 40
M71GL/L168HF	$14\,000 \pm 2000$	$13\,700 \pm 1700$	1150 ± 50
M71GL/L104EV	5800 ± 2500	5000 ± 2000	1260 ± 150
M71GL/M214LH	$10\,000 \pm 2800$	3600 ± 1900	1600 ± 300

The dependence of k_{obs} and the quantum yield of triplet formation on a weak magnetic field are similar in M71GL/L168HF and M71GL (Figures 4 and 5). The temperature dependence of k_{obs} at 8 T shown in Figure 8 fits to a single exponential with a slope of 1020 cm^{-1} ; thus, ΔH° between ^3P and $\text{P}^+\text{H}_\text{L}^-$ is about 200 cm^{-1} smaller in this mutant than in M71GL. Assuming that the singlet–triplet splitting remains the same in the M71GL/L168HF mutant and taking the energy of ^1P in M71GL/L168HF to be $11\,400 \text{ cm}^{-1}$, ΔH° for initial electron transfer is 2480 cm^{-1} , an increase of 210 cm^{-1} relative to the value derived for M71GL from the temperature-dependent data. k_{S} has not been explicitly measured; however, the decay of the bleach of P in Q-depleted RCs of the L168HF mutant following excitation by a 5-ns pulse was measured to be $3.8 \times 10^7 \text{ s}^{-1}$,³³ which is similar to the value for R26 RCs. The triplet yield at zero magnetic field was estimated by using samples with the same absorption at 532 nm and measuring the initial bleach of the P band at room temperature corrected for the transmission prior to the excitation pulse at the probe wavelength. The value is about 25% less in the M71GL/L168HF mutant than in M71GL, taking $\Phi_{3\text{P}}(B=0) = 0.32$ for M71GL and $\Phi_{3\text{P}}(B=0) = 0.25 \pm 0.05$ in the M71GL/L168HF mutant. The smaller preexponential derived from the fit of the temperature-dependent data in Figure 8 is consistent with the smaller value of $\Phi_{3\text{P}}(B=0)$ estimated for L168HF.

The magnetic-field-dependent data for M71GL/L168HF fit well to a straight line with slope $13\,700 \text{ s}^{-1}$. With k_{S} estimated as $4.9 \times 10^7 \text{ s}^{-1}$ and $\Phi_{3\text{P}}(B=0)$ estimated as 0.25, the slope of the fit to the magnetic-field-dependent data translates to ΔG° for $^3\text{P} \rightarrow \text{P}^+\text{H}_\text{L}^-$ of $1150 \pm 50 \text{ cm}^{-1}$, corresponding to ΔG° for $^1\text{P} \rightarrow \text{P}^+\text{H}_\text{L}^-$ of $2350 \pm 50 \text{ cm}^{-1}$. This is an increase of $240 \pm 50 \text{ cm}^{-1}$ relative to the value derived for M71GL, and again $\Delta G^\circ \approx \Delta H^\circ$.

The P/P^+ midpoint potential in L168HF decreases by $90 \pm 10 \text{ meV}$ relative to wild-type, a change of $725 \pm 80 \text{ cm}^{-1}$.^{19,20} Assuming that the mutation does not affect $\text{H}_\text{L}/\text{H}_\text{L}^-$, this change in the redox potential of P could translate directly to a change in the $^1\text{P} \rightarrow \text{P}^+\text{H}_\text{L}^-$ free energy difference, which might be expected to significantly affect the rate of primary charge separation. Nevertheless, the L168HF mutant has an electron-transfer lifetime that is almost identical to that of wild-type at room temperature (3.6 vs 3.8 ps for WT).¹⁹ The change in ΔG° that we measure is substantially smaller than the value predicted from the redox potential shift. Delayed fluorescence has been measured for L168HF, but the analysis of the data is problematic because the decay component of long-lived fluorescence that in WT is most convincingly assigned to $\text{P}^+\text{H}_\text{L}^-$ decay (i.e., due to its magnetic field dependence) is absent in the L168HF mutant.¹⁹ Murchison et al. speculated that the disappearance of the longest-lived delayed fluorescence component indicates an increase in the equilibrium constant favoring the forward reaction, suggesting an increase in the free energy difference between ^1P and $^1(\text{P}^+\text{H}_\text{L}^-)$.

By assuming that the ^1P – ^3P energy difference is the same as in WT, the energies of ^1P and ^3P both increase by approximately 200 cm^{-1} , so the observation from the triplet decay experiments that the free energy of charge separation also increases by about 200 cm^{-1} leads to the unexpected result that

the energy of the $\text{P}^+\text{H}_\text{L}^-$ state relative to the ground state in M71GL/L168HF is nearly identical to that in M71GL. In this scenario, the increase in the free energy difference between ^1P and $^1(\text{P}^+\text{H}_\text{L}^-)$ in M71GL/L168HF appears to be due entirely to the 200 cm^{-1} shift of the P absorption band to higher energy in the double mutant and not to the change in the redox potential of P. We stress that this last conclusion depends on the assumption that the singlet–triplet splitting in P is unchanged by the L168HF mutation. The data show that the energy difference between ^3P and $^3(\text{P}^+\text{H}_\text{L}^-)$ is smaller in L168HF; a direct measurement of the phosphorescence spectrum of ^3P in this mutant is needed to ascertain the true singlet–triplet splitting.

M71GL/L104EV. The L104EV mutation removes a hydrogen-bonding group near the ring V keto group in H_L . Resonance Raman,⁴⁴ infrared,⁴⁵ and ENDOR⁴⁶ experiments suggest that the native glutamic acid at position L104 interacts with the bacteriopheophytin in the H_L binding site, probably through a hydrogen bond. Removal of the L104 hydrogen bond is expected to raise the free energy of $\text{P}^+\text{H}_\text{L}^-$ as H_L becomes more difficult to reduce.⁴⁷ The hydrogen bond at L104E results in a red shift of the Q_X absorption of H_L , making the two bacteriopheophytin chromophores spectrally resolvable at low temperature (Figure 3). In the M71GL/L104EV mutant, the Q_X bacteriopheophytin bands overlap, and the Q_Y region of the H band becomes sharper. This is similar to what has been reported previously for the L104EL mutation in *Rb. capsulatus*²¹ and the L104EV mutation in *Rb. sphaeroides*.⁴⁷

k_{obs} and $\Phi_{3\text{P}}$ for M71GL/L104EV have little dependence on weak applied fields unlike in M71GL (Figures 4 and 5), whereas $\Phi_{3\text{P}}$ changes upon application of a high magnetic field much like M71GL (Figure 6). The temperature dependence of k_{obs} for M71GL/L104EV at 8 T fits to a single exponential with a slope of 1360 cm^{-1} , that is, the ^3P – $\text{P}^+\text{H}_\text{L}^-$ enthalpy gap is larger than in M71GL. The energy of ^3P should be unaffected by the L104EV mutation because the change is far from P and there is no effect on the Q_Y absorption of P. Thus, ΔH° for $^1\text{P} \rightarrow ^1(\text{P}^+\text{H}_\text{L}^-)$ from the temperature-dependent data is 2140 cm^{-1} , a decrease of 130 cm^{-1} relative to M71GL. The magnetic-field-dependent data for M71GL/L104EV are noisy but can be fit to a line with a slope of 5000 s^{-1} . The initial bleach amplitude at zero field and room temperature indicates that the triplet yield in M71GL/L104EV is 40–60% smaller than in M71GL, the uncertainty being due to the low triplet yield and large difference in absorption at 532 nm. A possible explanation for the low triplet yield is that k_{S} has increased; however, there is no evidence for this using the $\text{P}^+\text{H}_\text{L}^- \rightarrow \text{P}^+\text{Q}_\text{A}^-$ vs $\text{P}^+\text{H}_\text{L}^- \rightarrow$ ground state competition in *Rb. sphaeroides* as a metric.³⁴ Using the same value for k_{S} as in R26 and approximating $\Phi_{3\text{P}}(B=0)$ for M71GL/L104EV as 0.16 ± 0.05 , we obtain an approximate value for ΔG° for $^3\text{P} \rightarrow ^3(\text{P}^+\text{H}_\text{L}^-)$ of $1260 \pm 150 \text{ cm}^{-1}$. From this value, the calculated ΔG° for initial electron transfer is $2240 \pm 150 \text{ cm}^{-1}$. With the large uncertainty in ΔG° , it is not possible to offer more definitive information on the entropy at this time.

The redox potential of the H_L chromophore in situ in L104EV has not been measured. Room-temperature delayed fluorescence for the L104EV mutant in Q_A -containing *Rb. sphaeroides* suggests that the free energy of charge separation decreases by

about 250–320 cm⁻¹ relative to wild-type.³⁴ Unfortunately, the magnetic field dependence was not reported for this mutant, so it not clear that the measured delayed fluorescence arises from ¹P re-formation from the radical pair. The decrease in ΔH° for charge separation in M71GL/L104EV relative to M71GL that we measure is consistent with the direction of change measured by delayed fluorescence, but the magnitude of the change is substantially smaller.

The energetic effects of the L104EV mutation can also be measured by resonance Stark spectroscopy on the B_L absorption band.^{48,49} This spectroscopic observable arises from the effect of an applied electric field on the B_L* → B_L⁺H_L⁻ electron-transfer reaction. Among other electron-transfer parameters, changes in the driving force can be obtained. Assuming that only H_L is affected by the L104EV mutation, the energetic shift of B_L⁺H_L⁻ in L104EV can be compared to the energetic shift of P⁺H_L⁻ determined from triplet decay kinetics as they share the same energetic perturbation.⁵⁰ Both resonance Stark spectroscopy from our laboratory⁵¹ and the ³P decay measurements presented here are consistent with an increase in the energy of the charge-separated states in L104EV relative to that in wild-type. The resonance Stark effect in the L104EV mutant is small and difficult to resolve, but the extrapolated energy of B_L⁺H_L⁻ in L104EV is at least 300 cm⁻¹ larger than in wild-type. This is larger than the change in P⁺H_L⁻ as measured by triplet decay. The source of this discrepancy is not known and is discussed below. We note that the states and the underlying processes measured by each methodology are different and that both methods require multiple assumptions to extract energetics from the observables.

M71GL/M214LH. In M71GL/M214LH, the bacteriopheophytin in the H_L binding site is replaced by a bacteriochlorophyll. This improves the spectral resolution in the Q_Y region (Figure 3), and because bacteriochlorophyll is more difficult to reduce in vitro, this change is expected to perturb the energetics of initial electron transfer. Because M214 is far from the special pair, the energies of ¹P and ³P are not expected to change in the M71GL/M214LH mutant relative to M71GL, and the P-band Q_Y transition is unaffected (Figure 2).

Triplet yield and decay in M71GL/M214LH depend weakly on a small, applied magnetic field (Figures 4 and 5). The observed $\Phi_{3P}(B=8)/\Phi_{3P}(B=1)$ ratios for M71GL and M71GL/M214LH are the same within experimental error, with values of about 3 (Figure 6). Within the framework of the scheme in Figure 2 and in the high-field (>1 T) limit, triplet yields can be calculated using the equation⁵²

$$\Phi_{3P}(B) = \frac{k_T}{k_T + k_S} \left(\frac{\omega^2}{\omega^2 + \kappa^2} \right) \quad (5)$$

where

$$\omega = \frac{\Delta g \beta B}{\hbar} \quad (6)$$

and

$$\kappa^2 = k_S k_T + \frac{4\Delta E^2 k_S k_T}{(k_S + k_T)^2} \quad (7)$$

where β is the Bohr magneton, B is the applied magnetic field, \hbar is Planck's constant divided by 2π , and ΔE is the splitting between the S and T₀ states of the P⁺H_L⁻ radical pair. With the same values of Δg (0.001), ΔE (7 G), and k_T (5×10^8 s⁻¹) for these mutants, but assuming that k_S is 4.9×10^7 s⁻¹ for

M71GL and 1×10^9 s⁻¹ for M71GL/M214LH, we calculate that $\Phi_{3P}(B=8)/\Phi_{3P}(B=1)$ should be 32 for M71GL/M214LH and 4 for M71GL. Thus, the experimental results suggest the M214LH mutation might affect k_T , ΔE , or Δg , in addition to k_S .

Fitting the temperature-dependent data to an exponential results in a ΔH° value for ³P → ³(P⁺β_L⁻) of 1440 cm⁻¹. Combining this value with the energies of ³P and ¹P results in ΔH° for ¹P → ¹(P⁺β_L⁻) of 2060 cm⁻¹ for this mutant, 210 cm⁻¹ less than the value obtained for M71GL. This difference is similar in magnitude to the decrease in enthalpy measured in M71GL/L104EV.

Whereas k_S can be estimated for M214LH because singlet charge recombination to the ground state is so dominant in this mutant, $\Phi_{3P}(B=0)$ has not been reported. There are two ways to estimate $\Phi_{3P}(B=0)$ in M71GL/M214LH. We can compare the initial bleach of P at room temperature in M71GL/M214LH with that of M71GL, in which case we find that $\Phi_{3P}(B=0)$ is approximately a factor of 15 less in the double mutant than in M71GL, or about 0.02. Alternatively, the preexponential derived from the fit to the M71GL/M214LH data is found to be 3 times larger than the preexponential for M71GL. From eq 1, the preexponential is equal to $^{1/3}k_S\Phi_{3P}e^{\Delta S^\circ/k_B}$. Then assuming that k_S is 20 times greater in M71GL/M214LH than in M71GL and provided that ΔS° is similar in M71GL and M71GL/M214LH, $\Phi_{3P}(B=8)$ is about 7 times less for M71GL/M214LH than for M71GL under the same conditions. We measure $\Phi_{3P}(B=8)/\Phi_{3P}(B=0)$ in M71GL as 1.7, suggesting that, for M71GL/M214LH, $\Phi_{3P}(B=8) \approx 0.08$. In M71GL/M214LH, $\Phi_{3P}(B=8)/\Phi_{3P}(B=0)$ is about 2.3, suggesting that, for M71GL/M214LH at room temperature, $\Phi_{3P}(B=0) \approx 0.03$. This low triplet yield of course relates directly to the difficulty of measuring the triplet decay in M71GL/M214LH.

The magnetic-field-dependent data for M71GL/M214LH have a huge uncertainty because of the small triplet yield. The best fit to a line gives a slope of 3600 ± 1900 s⁻¹. Combining this result with the value of k_S for M214LH and a range of values for the zero-field $\Phi_{3P}(B=0) = 0.03 \pm 0.02$ gives ΔG° for ³P → ³(P⁺β_L⁻) of 1600 ± 300 cm⁻¹, resulting in ΔG° for ¹P → ¹(P⁺β_L⁻) of 1900 ± 300 cm⁻¹ for M71GL/M214LH, 210 ± 300 cm⁻¹ less than in M71GL. Many approximations were made in this estimate of ΔG° : the sign of the change relative to M71GL is what is expected, and ΔG° is in the same range as ΔH° .

Although the midpoint oxidation potential of P in M214LH has not been reported, the mutation is far enough away from the special pair that it should be unaffected. The reduction potential of bacteriochlorophyll *a* in CH₂Cl₂ has been measured to be -850 meV,²⁹ and this value would predict that P⁺β_L⁻ is only 270–350 cm⁻¹ below ¹P in M71GL/M214LH. Delayed fluorescence has been reported for the M214LH mutant, indicating that the free energy change associated with charge transfer is 600 ± 200 cm⁻¹, although the magnetic field dependence of the delayed fluorescence components was not measured to verify that the fluorescence is due to recombination from the radical pair state.²²

Assuming that only H_L is affected by the M214LH mutation, we can directly compare the energy shifts extracted from resonance Stark spectroscopy on the B_L absorption⁵¹ to those obtained from the ³P decay data, as was done for L104EV. Both resonance Stark spectroscopy and ³P decay suggest that the energy of the charge-separated states is increased in M214LH relative to that in WT. The resonance Stark effect for B_L in the M214LH mutant is small and difficult to resolve; nonetheless,

the extrapolated energy of $B_L^+\beta_L^-$ appears to be greater than that in L104EV. Thus, although the direction of the change is the same, as with L104EV, the resonance Stark data suggest a larger change than the 3P decay data.

Summary and Issues. An analysis of the temperature dependence of the 3P decay in high magnetic fields can provide quantitative information on the energetics of $P^+H_L^-$ relative to 3P . Experimental information on the energetics in situ is invariably obtained by indirect approaches, and each approach has specific assumptions and associated limitations. As discussed earlier, there appears to be a consistent difference in the energetics obtained by delayed fluorescence and by the activation energy of the triplet decay. Volk et al. have discussed the possibility that there is a distribution of $P^+H_L^-$ energies, and this possibility is reasonable given the large change in charge distribution associated with charge separation.⁴³ On the other hand, the RC is exquisitely designed to perform efficient charge separation, even at low temperature, so an alternative view is that the RC protein has evolved specifically to accommodate the charge-separated species, i.e., the distribution might be quite homogeneous (this would have little effect on the neutral ground state).

If an inhomogeneous distribution of $P^+H_L^-$ energies were relevant for the delayed fluorescence and triplet decay measurements, then one would expect that the energies extracted by each method would be weighted toward the top and bottom, respectively, of this distribution. Because the triplet decay experiments sample the lower fraction of the radical pair, the data would underestimate the enthalpy difference between 3P and $P^+H_L^-$, leading to an overestimate of the enthalpy difference between 1P and $P^+H_L^-$. If the width of the energetic inhomogeneity is the same for all mutants but the center of the distribution shifts systematically, the triplet decay would underestimate the enthalpy difference for each mutant, but the relative enthalpy difference between mutants should reflect the actual enthalpy difference between the mutants. The magnitude of the systematic underestimate depends on the energetic width of the radical ion pair inhomogeneity. Ognodnik et al. used a Gaussian distribution of free energies and estimated a width of 800 cm^{-1} .⁷ Resonance Stark experiments from our laboratory are interpreted using a distribution of coupled energies (in that case, for the $B_L^+H_L^-$ state) that is on the order of 1000 cm^{-1} . Unfortunately, this parameter is not well determined by the resonance Stark data obtained to date; however, the data are totally inconsistent with a spread less than about 500 cm^{-1} . It is interesting that the resonance Stark data give energy shifts with mutation that are intermediate between the values estimated from delayed fluorescence and triplet decay data. The resonance Stark effect depends both on the width of the distribution (assumed to be Gaussian) and on its peak value, so this might ultimately prove to be the best method for extracting true energies. Unfortunately, resonance Stark effects are not observed for the excitation of P itself for reasons discussed in the original papers.^{48,49,51} Nonetheless, in cases where the perturbation is shared, such as those for H_L/H_L^- , direct comparisons are possible.

Acknowledgment. We thank the Stanford Free Electron Laser Center, supported by the Air Force Office of Scientific Research (Grant F49620-00-1-0349), for generous use of their Spectromag system and the NSF Biophysics Program for ongoing support of this research.

References and Notes

(1) Chidsey, C. E. D.; Takiff, L.; Goldstein, R.; Boxer, S. G. *Proc. Natl. Acad. Sci. U.S.A.* **1985**, *82*, 6850–6854.

(2) Schenck, C. C.; Blankenship, R. E.; Parson, W. W. *Biochim. Biophys. Acta* **1982**, *680*, 44–59.

(3) Woodbury, N. W.; Parson, W. W. *Biochim. Biophys. Acta* **1984**, *767*, 345–361.

(4) Woodbury, N. W.; Parson, W. W. *Biochim. Biophys. Acta* **1986**, *850*, 197–210.

(5) Ognodnik, A. *Biochim. Biophys. Acta* **1990**, *1020*, 65–71.

(6) Pelloquin, J. M.; Williams, J. C.; Lin, X.; Alden, R. G.; Taguchi, A. K. W.; Allen, J. P.; Woodbury, N. W. *Biochemistry* **1994**, *33*, 8089–8100.

(7) Ognodnik, A.; Keupp, W.; Volk, M.; Aumeier, G.; Michel-Beyerle, M. E. *J. Phys. Chem.* **1994**, *98*, 3432–9.

(8) Goldstein, R. A.; Takiff, L.; Boxer, S. G. *Biochim. Biophys. Acta* **1988**, *934*, 253–263.

(9) Takiff, L.; Boxer, S. G. *Biochim. Biophys. Acta* **1988**, *932*, 325–334.

(10) Ridge, J. P.; van Brederode, M. E.; Goodwin, M. G.; van Grondelle, R.; Jones, M. R. *Photosynth. Res.* **1999**, *59*, 9–26.

(11) The notation P^+I^- was used in the earlier literature, as the nature of the intermediate electron acceptor I was not certain. It is generally agreed that the radical pair whose magnetic exchange interaction is small enough to allow singlet–triplet mixing by hyperfine fields and g factor differences is $P^+H_L^-$, not $P^+B_L^-$. There is no definitive proof for this, and the observation that the mutations near B_L can affect 3P decay suggest that $P^+B_L^-$ might be involved. We will use the notation $P^+H_L^-$ to describe operationally the state whose fate can be manipulated by a magnetic field, noting this caveat.

(12) Roelofs, M. G.; Chidsey, C. E. D.; Boxer, S. G. *Chem. Phys. Lett.* **1982**, *87*, 582–588.

(13) Werner, H.; Schulten, K.; Weller, A. *Biochim. Biophys. Acta* **1978**, *502*, 255–268.

(14) Haberkorn, R.; Michel-Beyerle, M. E. *Biophys. J.* **1979**, *26*, 489–498.

(15) Chidsey, C. E. D.; Roelofs, M. G.; Boxer, S. G. *Chem. Phys. Lett.* **1980**, *74*, 113–118.

(16) Goldstein, R. A.; Boxer, S. G. *Biophys. J.* **1987**, *51*, 937–936.

(17) To circumvent the problems of nuclear spin polarization, we attempted to excite 3P directly in Q-depleted M71GL RCs, using an optical parametric oscillator (OPO) as an excitation source. We scanned the output of the OPO between 1200 and 1400 nm without observing any measurable P ground-state bleach signal with lock-in detection. Because the molar extinction coefficient of the B band is known, we used 800-nm excitation of the B band as a standard to estimate that the molar extinction coefficient for triplet absorption must be less than 10.

(18) We note that the interconversion between $^1(P^+H_L^-)$ and $^3(P^+H_L^-)$ is also critical for delayed fluorescence measurements, because in those experiments the delayed fluorescence arises from equilibration between $^1(P^+H_L^-)$ and 1P . Delayed fluorescence measurements and triplet decay experiments are thus both plagued to some degree by nuclear spin polarization.

(19) Murchison, H. A.; Alden, R. G.; Allen, J. P.; Pelloquin, J. M.; Taguchi, A. K. W.; Woodbury, N. W.; Williams, J. C. *Biochemistry* **1993**, *32*, 3498–505.

(20) Lin, X.; Murchison, H. A.; Nagarajan, V.; Parson, W. W.; Williams, J. C.; Allen, J. P. *Proc. Natl. Acad. Sci. U.S.A.* **1994**, *91*, 10265–10269.

(21) Bylina, E. J.; Kirmaier, C.; McDowell, L.; Holten, D.; Youvan, D. C. *Nature* **1988**, *336*, 182–184.

(22) Kirmaier, C.; Gaul, D.; Debey, R.; Holten, D.; Schenck, C. C. *Science* **1991**, *251*, 922–926.

(23) Goldsmith, J. O.; Boxer, S. G. *Biochim. Biophys. Acta* **1996**, *1276*, 171–175.

(24) Okamura, M. Y.; Isaacson, R. A.; Feher, G. *Proc. Natl. Acad. Sci. U.S.A.* **1975**, *72*, 3491–3495.

(25) Boxer, S. G.; Chidsey, C. E. D.; Roelofs, M. G. *Proc. Natl. Acad. Sci. U.S.A.* **1982**, *79*, 4632–4636.

(26) Mueh, F.; Lubitz, W. Personal communication; Max-Planck-Institute für Strahlenchemie, Mülheim an der Ruhr, Germany, 2002.

(27) Fajer, J.; Borg, D. C.; Forman, A.; Dolphin, D.; Felton, R. H. *J. Am. Chem. Soc.* **1973**, *95*, 2739–2741.

(28) Fajer, J.; Forman, A.; Davis, M. S.; Spaulding, L. D.; Brune, D. C.; Felton, R. H. *J. Am. Chem. Soc.* **1977**, *99*, 4134–4140.

(29) Fajer, J.; Brune, D. C.; Davis, M. S.; Forman, A.; Spaulding, L. D. *Proc. Natl. Acad. Sci. U.S.A.* **1975**, *72*, 4956–4960.

(30) Lubitz, W.; Lenzian, F.; Mobius, K. *Chem. Phys. Lett.* **1981**, *84*, 33–38.

(31) Budil, D. E.; Gast, P.; Chang, C. H.; Schiffer, M.; Norris, J. *Annu. Rev. Phys. Chem.* **1987**, *38*, 561–583.

(32) Schenck, C. C.; Mathis, P.; Lutz, M. *Photochem. Photobiol.* **1984**, *39*, 407–417.

(33) Tang, C.-K.; Williams, J. C.; Taguchi, A. K. W.; Allen, J. P.; Woodbury, N. W. *Biochem.* **1999**, *38*, 8794–8799.

(34) Kirmaier, C.; Laporte, L.; Schenck, C. C.; Holten, D. *J. Phys. Chem.* **1995**, *99*, 8910–8917.

- (35) Chidsey, C. E. D.; Kirmaier, C.; Holten, D.; Boxer, S. G. *Biochim. Biophys. Acta* **1984**, *766*, 424–437.
- (36) Parson, W. W. In *Protein Electron Transfer*; Bendall, D. S., Ed.; BIOS Scientific Publishers Ltd: Oxford, U.K., 1996; Vol. 1; pp 125–160.
- (37) Moss, D. A.; Leonhard, M.; Bauscher, M.; Mantele, W. *FEBS Lett.* **1991**, *283*, 33–36.
- (38) Williams, J. C.; Alden, R. G.; Murchison, H. A.; Peloquin, J. M.; Woodbury, N. W.; Allen, J. P. *Biochemistry* **1992**, *31*, 11029–37.
- (39) Nagarajan, V.; Parson, W. W.; Davis, D.; Schenck, C. C. *Biochemistry* **1993**, *32*, 12324–12336.
- (40) Allen, J. P.; Artz, K.; Lin, X.; Williams, J. C.; Ivancich, A.; Albouy, D.; Mattioli, T. A.; Fetsch, A.; Kuhn, M.; Lubitz, W. *Biochemistry* **1996**, *35*, 6612–6619.
- (41) Dutton, P. L.; Kaufmann, K. J.; Chance, B.; Rentzepis, P. M. *FEBS Lett.* **1975**, *60*, 275–280.
- (42) Holzwarth, A. R.; Müller, M. G. *Biochemistry* **1996**, *35*, 11820–11831.
- (43) Volk, M.; Aumeier, G.; Langenbacher, T.; Feick, R.; Ogrodnick, A.; Michel-Beyerle, M.-E. *J. Phys. Chem. B* **1998**, *102*, 735–751.
- (44) Bocian, D. F.; Boldt, N. J.; Chadwick, B. W.; Frank, H. A. *FEBS Lett.* **1987**, *214*, 92–96.
- (45) Nabedryk, E.; Andrianambinintsoa, S.; Mantele, W.; Breton, J. In *The Photosynthetic Bacterial Reaction Center: Structure and Dynamics*; Breton, J., Vermeglio, A., Eds.; Plenum Press: New York, 1988; pp 237–250.
- (46) Feher, G.; Isaacson, R. A.; Okamura, M. Y.; Lubitz, W. In *The Photosynthetic Bacterial Reaction Center*; Breton, J., Vermeglio, A., Eds.; Plenum Press: New York, 1988; pp 229–235.
- (47) Kirmaier, C.; Laporte, L.; Schenck, C. C.; Holten, D. *J. Phys. Chem.* **1995**, *99*, 8903–8909.
- (48) Zhou, H. L.; Boxer, S. G. *J. Phys. Chem. B* **1998**, *102*, 9139–9147.
- (49) Zhou, H. L.; Boxer, S. G. *J. Phys. Chem. B* **1998**, *102*, 9148–9160.
- (50) The distance of the cation, P^+ or B_L^+ , from H_L^- might alter the energetics somewhat.
- (51) Treynor, T.; Boxer, S. G., manuscript in preparation.
- (52) Goldstein, R. A. Ph.D. Thesis, Stanford University, Stanford, CA, 1988.